Internal Point Solutions for Displacements and Stresses in 3D Anisotropic Elastic Solids Using the Boundary Element Method

Y.C. Shiah[1], C. L. Tan[2] and R.F. Lee[1]

Abstract: In this paper, fully explicit, algebraic expressions are derived for the first and second derivatives of the Green's function for the displacements in a three dimensional anisotropic, linear elastic body. These quantities are required in the direct formulation of the boundary element method (BEM) for determining the stresses at internal points in the body. To the authors' knowledge, similar quantities have never previously been presented in the literature because of their mathematical complexity. Although the BEM is a boundary solution numerical technique, solutions for the displacements and stresses at internal points are sometimes required for some engineering applications. To this end, the availability of the derivatives of the fundamental solution in closed, algebraic form enables their implementation into an existing BEM code in a relatively straightforward manner. Some examples are presented to demonstrate the veracity of these expressions and their successful implementation for determining interior point solutions in 3D general anisotropic elastostatics in BEM.

Keywords: Boundary element method, Green's functions, boundary integral equations, Somigliana's identity, anisotropic elasticity, Stroh's eigenvalues.

1 Introduction

A distinctive feature of the boundary element method (BEM), as a computational tool for engineering stress analysis of elastic bodies, is that only the boundary or the surface of the numerical solution domain needs to be modeled. With this technique, it is also well known that interior point solutions for the displacements and the stresses at an interior point are obtained as a secondary exercise in the analysis, only if required. It involves the numerical evaluation of the Somigliana's identities, after the boundary integral equation (BIE) has been solved for all the un-

---

[1] Dept. of Aerospace and Systems Engineering, Feng Chia University, Taichung, Taiwan, R.O.C.

[2] Dept. of Mechanical & Aerospace Engineering, Carleton University, Ottawa, Canada K1S 5B6

known displacements and tractions on the surface of the domain. In the integrals of these identities, the integrands contain terms with up to second order derivatives of the Green's function, or fundamental solution, for the displacements of the elastic problem.

The Green's function for displacements and that for tractions are necessary items for the direct formulation of the BEM for elastic stress analysis. For 3D general anisotropic solids, the Green's function for displacements has been presented many years ago by Lifshitz and Rosenzweig (1947). It was expressed as a contour integral around a unit circle on an oblique plane at the field point and the integrand contains the Christoffel tensor defined in terms of the material elastic constants. However, in the development of the BEM to treat such bodies, the numerical evaluation of these fundamental solutions has remained a subject of investigation over the past few decades; see, e.g. Wilson and Cruse (1978), Sales and Gray (1998), Pan and Yuan (2000), Tonon *et al* (2001), Phan *et al* (2004), Wang and Denda (2007), Shiah *et al* (2008), Tan *et al* (2009). This is because of their mathematical complexity. In the BEM formulation presented by the present authors very recently, Shiah *et al* (2008) and Tan *et al* (2009), the fundamental solutions employed in the BIE are expressed in exact, algebraic, real-variable explicit forms, unlike those used by the other authors previously. They were derived by Ting and Lee (1997) for displacements, and Lee (2003) for their first derivatives which are then utilized for the derivation of the traction solution, respectively. These Green's functions were used for the first time in a BEM formulation for general anisotropy. Because of their algebraic forms, they can be numerically evaluated in a fairly straightforward manner. Their implementation into an existing BEM code, based on the quadratic isoparametric element formulation which had been developed for 3D isotropic elastostatics, was also carried out without any difficulty. It was, however, discovered that, when computing the kernels of the BIE, a significant proportion of the computational effort is spent on evaluating high-order tensor terms which appear in Lee's (2003) solution. Following the collaborative work in Shiah *et al* (2008), Lee (2009) re-examined her solution and showed how a simpler analytical form for the first derivatives of the displacement Green's function could be obtained without the high-order tensors. This can be achieved by carrying out the partial differentiation in a spherical coordinate system as an intermediate step instead of the direct differentiation with respect to the Cartesian coordinates. In the paper, however, the explicit expressions are presented only for the special case of transverse isotropy. As a result of this development, the present authors derived the corresponding fully explicit forms of the solution for the displacement first derivatives in general anisotropy. Their validity and superior efficiency of using these alternative, fully explicit forms of the fundamental solutions in the BIE is demonstrated very recently in Shiah *et al* (2010); the

expressions, unfortunately, were not presented in the conference paper because of the page limit.

Of significance to note too is that Lee's (2009) revised approach also lends itself readily to obtaining higher order derivatives of the Green's function for the displacements without the need to introduce high-order tensor quantities. The present authors have further derived the expressions, in fully explicit algebraic forms, of the second derivatives of the fundamental solution. This enables the extension of the BEM for the numerical determination of the displacements and stresses at an interior point of a 3D generally anisotropic solid. To the authors' knowledge, this development has never been reported previously in the literature and is the focus of the present paper. Although the BEM is a boundary solution technique for engineering analysis, interior point displacements and stresses are sometimes required, such as in the evaluation of contour integrals within the body around a crack front for determining fracture parameters in fracture mechanics analysis.

It should be remarked here that other algorithms for computing the higher-order derivatives of the displacement Green's function for BEM implementation have been presented before. For example, they were recently computed in a BEM formulation by Benedetti *et al* (2009). However, the focus of their work was on the development of a fast dual BEM for 3D anisotropic crack problems and not on the development of new forms of the Green's function, or the BEM computation of internal point solutions. The Green's function they used was that by Lifshitz and Rosenzweig (1947), and the approximations for the numerical values of this Green's function and its derivatives were obtained using interpolation, following the approach originally developed by Wilson and Cruse (1978). In that scheme, a relatively large database of numerically evaluated point load solutions and their derivatives is first established for the given material being analyzed. When performing the integration of the kernel functions over the boundary elements during the collocation process, the required values of the Green's function and its derivatives are obtained by interpolation of the pre-calculated ones retrieved from the database. The possible difficulty of maintaining the accuracy of the interpolated values using this approach, particularly for cases of highly anisotropic materials, was noted by Schclar (1994), and Sales and Gray (1998). The latter, and Phan *et al* (2004), have also presented an alternative numerical scheme using residue calculus that offers significant improvements in computational efficiency over the Wilson-Cruse approach. It should be emphasized again, however, that in all these work described, the fundamental solutions are not of closed-form, unlike those used in the present study. It should also be noted that very recently, Buroni and Saez (2010) have derived a general algebraic expression for the second-order derivatives of the Green's function following Lee's (2003) original approach. As expected, it contains

terms that are 10th-order tensors which were not evaluated for the explicit algebraic forms in the paper, however. The avoidance of these high-order tensors is a key motivation for the formulation used in the present work; this has been discussed earlier.

Because of their explicit algebraic form, it is relatively straightforward to implement the Green's function and its derivatives used in the present work into an existing BEM code which had been developed for three-dimensional isotropic elastostatics. This has been successfully achieved; there being no specific issue that requires special attention in this regard. Thus, in what follows, the numerical formulation of the BEM will not be discussed as it is well established in the literature. A review of the Green's function for displacements and its derivatives for a 3D anisotropic elastic body that are used in the present study is presented. The explicit expressions for the higher order derivatives of the Green's function, required for the determination of the stresses at an interior point of an anisotropic body, are derived in this study. Some examples are then presented to demonstrate their validity. The numerical solutions obtained are compared with those obtained using the FEM or by a finite difference approach.

2   Fundamental solutions of 3D anisotropic elasticity

The boundary integral equation (BIE), which relates the nodal displacements u_j and tractions t_j at the boundary S of the homogeneous elastic domain, is written in indicial notation as

$$C_{ij}u_i(P) + \int_S u_i(Q)T_{ij}(P,Q)dS = \int_S t_i(Q)U_{ij}(P,Q)dS \tag{1}$$

where the leading coefficient $C_{ij}(P)$ depends upon the local geometry of S at the source point P; $U_{ij}(P,Q) \equiv \mathbf{U}$, and $T_{ij}(P,Q)$ represent the fundamental solutions of displacements and tractions, respectively, in the x_i-direction at the field point Q due to a unit load in the x_j-direction at P in a homogeneous infinite body. Computation of the fundamental solution of displacements for generally anisotropic materials proposed in Ting and Lee (1997) has been discussed in Shiah *et al* (2008). It is presented here again for completeness.

Referring to Figure 1, let $\mathbf{n}$ and $\mathbf{m}$ be two mutually perpendicular unit vectors on the oblique plane at Q normal to the position vector $\mathbf{x}$; the vectors $[\mathbf{n}, \mathbf{m}, \mathbf{x}/r]$ forms a right-angle triad. By considering a spherical coordinate system as shown, the explicit form of the Green's function can be expressed as

$$U(\mathbf{x}) = \frac{1}{4\pi r}\frac{1}{|\boldsymbol{\kappa}|}\sum_{n=0}^{4}q_n\hat{\mathbf{\Gamma}}^{(n)}, \tag{2}$$
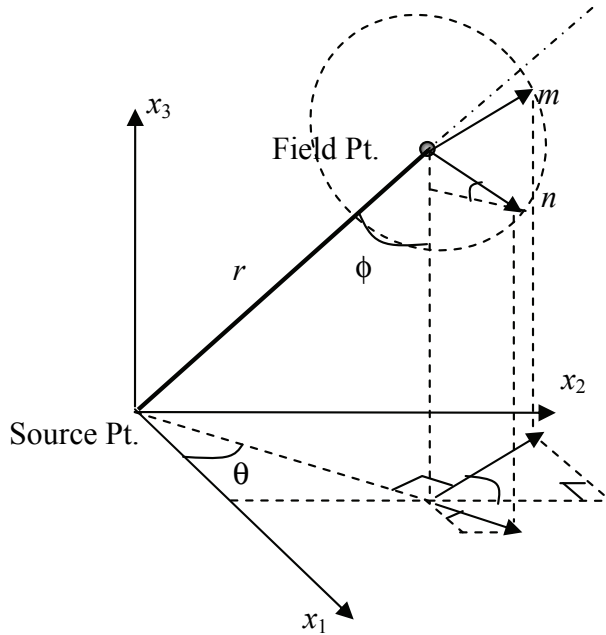
Figure 1: Unit circle on the oblique plane at the field point Q

where r represents the radial distance between the source point P and the field point Q; q_n, $\hat{\mathbf{\Gamma}}^{(n)}$, and $\boldsymbol{\kappa}$ are given by

$$q_n = \begin{cases} \frac{-1}{2\beta_1\beta_2\beta_3} \left[Re\left\{ \sum_{t=1}^{3} \frac{p_t^n}{(p_t - \bar{p}_{t+1})(p_t - \bar{p}_{t+2})} \right\} - \delta_{n2} \right] & for \ n = 0, 1, 2, \\ \frac{1}{2\beta_1\beta_2\beta_3} Re\left\{ \sum_{t=1}^{3} \frac{p_t^{n-2}\bar{p}_{t+1}\bar{p}_{t+2}}{(p_t - \bar{p}_{t+1})(p_t - \bar{p}_{t+2})} \right\} & for \ n = 3, 4, \end{cases} \tag{3a}$$

$$\hat{\Gamma}_{ij}^{(n)} = \tilde{\Gamma}_{(i+1)(j+1)(i+2)(j+2)}^{(n)} - \tilde{\Gamma}_{(i+1)(j+2)(i+2)(j+1)}^{(n)}, \quad (i,j = 1, 2, 3), \tag{3b}$$

$$\kappa_{ik} = C_{ijks}m_jm_s, \quad \mathbf{m} = (-\sin\theta, \cos\theta, 0). \tag{3c}$$

In Eq. (3a), the Stroh eigenvalues, p_i, are the roots of the sextic equation. They are complex for positive strain energy and appear as three pairs of complex conjugates. These quantities are expressed as

$$p_v = \alpha_v + i\beta_v, \beta_v > 0, (v = 1, 2, 3) \tag{4}$$

with an overbar on it denoting the corresponding conjugate. Also, in Eq. (3c), C_{ijks} are the stiffness coefficients of material. It has been demonstrated in Shiah

et al (2008) and Tan *et al* (2009) that the numerical evaluation of this Green's function is relatively straightforward; there is no issue that arises concerning its direct computation.

In addition to **U**, numerical evaluation of T_{ij} is also required in Eq. (1). This may be carried out as follows. First, the relationship between tractions and stresses, namely,

$$T_{ij} = \sigma_{ik}^{(j)} N_k, \tag{5}$$

is used, where $\sigma_{ik}^{(j)}$ are the stresses at a field point due to a unit concentrated force applied in the x_j direction at the source point, and N_k are components of the outward normal vector of the surface at Q. The generalized Hooke's law is then invoked, viz,

$$\sigma_{ik}^{(j)} = C_{ikmn} \left(U_{mj,n} + U_{nj,m} \right) / 2. \tag{6}$$

From Eqs.(5) and (6), it is clear that the 1st-order derivatives of **U** must first be obtained in order to evaluate the fundamental solution for stresses or tractions. This will be addressed next.

3 1st-order derivatives of the fundamental solution for displacements

In the earlier work by Lee (2003), the differentiation of the above Green's function is carried out directly in the Cartesian coordinate system. The derivatives so obtained can be expressed as

$$U_{ij,l} = \frac{1}{4\pi^2 r^2} \left[-\pi y_l H_{ij} + C_{pqrs} \left(y_s M_{lqiprj} + y_q M_{sliprj} \right) \right], \tag{7}$$

where y_i are the components of a unit position vector $\mathbf{y} = \mathbf{x}/r$ in the spherical coordinate system, expressed in terms of the spherical angles (θ, ϕ) defined in Figure 1; M_{ijklmn} can be shown to be as follows:

$$M_{ijklmn} = \frac{2\pi i}{|\kappa|^2} \sum_{t=1}^{3} \frac{1}{(p_t - p_{t+1})^2 (p_t - p_{t+2})^2}$$
$$\left[\Phi'_{ijklmn}(p_t) - 2\Phi_{ijklmn}(p_t) \left(\frac{1}{p_t - p_{t+1}} + \frac{1}{p_t - p_{t+2}} \right) \right]. \tag{8}$$

The full algebraic expression of Φ_{ijklmn} may be found in Shiah *et al* (2008) and Tan *et al* (2009). In the course of carrying out more extensive tests and analysis using

these fundamental solutions (Tan *et al*, 2009), it was discovered that a significant proportion of the computational effort is devoted to evaluating the terms in eq. (7) and eq. (8). Their evaluation involves numerous arithmetic operations due to the presence of the high-order tensors even though it is a relatively direct and simple exercise. In addition, in some instances of the case degenerate roots in transverse isotropy, it was found that serious truncation errors may occur in computing these derivatives; these errors may be easily rectified by using double precision arithmetic, however.

Lee (2009) revisited the problem and very recently re-derived $U_{ij,l}$ into a different algebraic form which removes the high-order tensors shown above. This was achieved by differentiating with respect to spherical coordinates as an intermediate step, separating the terms associated with the radial distance, and then applying the chain rule for the total derivative. Although the procedures are valid for the general case, as mentioned earlier, only the explicit expressions for transverse isotropy were presented in the paper. Those for the former are derived here following this approach. The 1st-order derivatives of displacements can be expressed in the spherical coordinate system as

$$U_{ij,l} = \frac{\partial U_{ij}}{\partial r}\frac{\partial r}{\partial x_l} + \frac{\partial U_{ij}}{\partial \theta}\frac{\partial \theta}{\partial x_l} + \frac{\partial U_{ij}}{\partial \varphi}\frac{\partial \varphi}{\partial x_l} \tag{9}$$

The partial derivatives of U_{ij} with respect to r, θ, and ϕ are given by

$$\frac{\partial U_{ij}}{\partial r} = \frac{-U_{ij}}{r}, \quad \frac{\partial U_{ij}}{\partial \theta} = \frac{I'_{ij} - J'_{ij}}{4\pi^2 r}, \quad \frac{\partial U_{ij}}{\partial \varphi} = \frac{I''_{ij} - J''_{ij}}{4\pi^2 r}, \tag{10}$$

where I'_{ij}, I'_{ij}, J''_{ij}, J''_{ij} can be expressed as

$$I'_{ij} = \frac{\pi}{|\boldsymbol{\kappa}|}\sum_{n=0}^{4} q_n \frac{\partial \hat{\Gamma}^{(n)}_{ij}}{\partial \theta}, \quad I''_{ij} = \frac{\pi}{|\boldsymbol{\kappa}|}\sum_{n=0}^{4} q_n \frac{\partial \hat{\Gamma}^{(n)}_{ij}}{\partial \varphi}, \tag{11a}$$

$$J'_{ij} = \frac{4\pi^2 r}{|\boldsymbol{\kappa}|}\frac{\partial |\boldsymbol{\kappa}|}{\partial \theta} U_{ij} + \frac{\pi}{|\boldsymbol{\kappa}|}\int_{-\infty}^{\infty} \frac{\hat{\Gamma}_{ij}(p) \cdot \partial f(p)/\partial \theta}{f(p)^2} dp, \tag{11b}$$

$$J''_{ij} = \frac{\pi}{|\boldsymbol{\kappa}|}\int_{-\infty}^{\infty} \frac{\hat{\Gamma}_{ij}(p) \cdot \partial f(p)/\partial \varphi}{f(p)^2} dp. \tag{11c}$$

In eq. (11b), $|\boldsymbol{\kappa}|$ can be shown to be given by

$$|\boldsymbol{\kappa}| = k_1 + \sum_{n=1}^{3}(k_{2n}\cos 2n\theta + k_{3n}\sin 2n\theta), \tag{12}$$

where the expressions for the coefficients are listed in Appendix A. It should be noted that, although $|\boldsymbol{\kappa}|$ may be computed using eq. (3c) directly, it is more efficient to use eq.(12) since its coefficients are related to the material properties and they need to be computed only once. In eq.(11b), $\partial |\boldsymbol{\kappa}| / \partial \theta$ can thus be obtained by direct differentiation to give

$$\frac{\partial |\boldsymbol{\kappa}|}{\partial \theta} = 2n \sum_{n=1}^{3} \left(-k_{2n} \sin 2n\theta + k_{3n} \cos 2n\theta \right). \tag{13}$$

In eq.(11b) and (11c), $f(p)$ is the sextic equation, written as

$$f(p) = p^6 + \sum_{m=0}^{5} \frac{\alpha_m(\theta, \varphi)}{\alpha_6(\theta, \varphi)} p^m, \tag{14}$$

the coefficients $\alpha_0(\theta, \varphi) \sim \alpha_6(\theta, \varphi)$ of which are given by

$$
\begin{aligned}
\alpha_0(\theta, \varphi) = {} & A_0 + \cos^6 \varphi \left(B_0 \cos 6\theta + C_0 \sin 6\theta \right) \\
& + \cos^5 \varphi \sin \varphi \left(D_0 \cos 5\theta + E_0 \sin 5\theta \right) \\
& + \sum_{k=0}^{1} \left\{ \begin{array}{l} \cos^4 \varphi \left[\cos 4\theta \left(F_{0k} \cos 2k\varphi \right) + \sin 4\theta \left(G_{0k} \cos 2k\varphi \right) \right] \\ + \cos^3 \varphi \sin \varphi \left[\cos 3\theta \left(H_{0k} \cos 2k\varphi \right) + \sin 3\theta \left(I_{0k} \cos 2k\varphi \right) \right] \end{array} \right\} \\
& + \sum_{k=0}^{2} \left\{ \begin{array}{l} \cos^2 \varphi \left[\cos 2\theta \left(J_{0k} \cos 2k\varphi \right) + \sin 2\theta \left(K_{0k} \cos 2k\varphi \right) \right] \\ + \sin \theta \sin 2\varphi \left[L_{0k} \cos 2k\varphi \right] \end{array} \right\} \\
& + \cos \theta \sum_{k=1}^{3} \left(M_{0k} \sin 2k\varphi + N_{0k} \cos 2k\varphi \right)
\end{aligned}
\tag{15a}
$$

$$
\begin{aligned}
\alpha_1(\theta, \varphi) = {} & \cos^5 \varphi \left(A_1 \cos 6\theta + B_1 \sin 6\theta \right) + \cos^4 \varphi \sin \varphi \left(C_1 \cos 5\theta + D_1 \sin 5\theta \right) \\
& + \sum_{k=0}^{1} \left\{ \begin{array}{l} \cos^3 \varphi \left[\cos 4\theta \left(E_{1k} \cos 2k\varphi \right) + \sin 4\theta \left(F_{1k} \cos 2k\varphi \right) \right] \\ + \cos^2 \varphi \sin \varphi \left[\cos 3\theta \left(G_{1k} \cos 2k\varphi \right) + \sin 3\theta \left(H_{1k} \cos 2k\varphi \right) \right] \end{array} \right\} \\
& + \sum_{k=0}^{2} \left\{ \cos \varphi \sin 2\theta \left[I_{1k} \cos 2k\varphi \right] + \sin \varphi \sin \theta \left[J_{1k} \cos 2k\varphi \right] \right\} \\
& + \sum_{k=1}^{3} \left\{ \cos \theta \left[K_{1k} \sin(2k-1)\varphi \right] + \cos 2\theta \left[L_{1k} \cos(2k-1)\varphi \right] \right\}
\end{aligned}
\tag{15b}
$$

$$\alpha_2(\theta,\varphi) = A_2 + \cos^4\varphi\,(B_2\cos6\theta + C_2\sin6\theta)$$
$$+\cos^3\varphi\sin\varphi\,(D_2\cos5\theta + E_2\sin5\theta)$$
$$+\sum_{k=1}^{2}\left\{\sin2\varphi\left[\begin{array}{c}\cos2\varphi\,(F_{2k}\cos(2k-1)\theta + G_{2k}\sin(2k-1)\theta)\\ +H_{2k}\cos(2k-1)\theta + I_{2k}\sin(2k-1)\theta\end{array}\right] \atop +\cos2k\varphi\sum_{m=0}^{2}K_{2km}\cos2m\theta + J_{2k}\cos2k\theta\right\},$$
$$+\sin2\theta\sum_{k=0}^{2}L_{2k}\cos2k\varphi + \cos^2\varphi\sin4\theta\sum_{k=0}^{1}M_{2k}\cos2k\varphi$$

$$(15c)$$

$$\alpha_3(\theta,\varphi) = \cos^3\varphi\,(A_3\cos6\theta + B_3\sin6\theta)$$
$$+\sum_{k=0}^{1}\cos\varphi\sin2\theta\,[D_{3k}\cos2k\varphi] + \sum_{k=1}^{2}\cos2\theta\,[C_{3k}\cos(2k-1)\varphi]$$
$$+\sin\varphi\left\{\begin{array}{l}\sum_{k=1}^{2}[E_{3k}\cos(2k-1)\theta + F_{3k}\sin(2k-1)\theta]\\ +\sum_{k=1}^{2}[\cos2\varphi\,(G_{3k}\cos(2k-1)\theta + H_{3k}\sin(2k-1)\theta)]\\ +\cos\varphi\left[\begin{array}{l}\cos\varphi\,(I_3\cos5\theta + J_3\sin5\theta)\\ +\sin\varphi\,(K_3\cos4\theta + L_3\sin4\theta)\end{array}\right]\end{array}\right\},\qquad(15d)$$

$$\alpha_4(\theta,\varphi) = A_4 + \sum_{k=1}^{3}\{B_{4k}\cos2k\theta + C_{4k}\sin2k\theta\}$$
$$+\cos2\varphi\left[D_4 + \sum_{k=1}^{6}(E_{4k}\cos k\theta + F_{4k}\sin k\theta)\right],\qquad(15e)$$

$$\alpha_5(\theta,\varphi) = \sum_{k=1}^{3}\left\{\begin{array}{l}\cos\varphi\,[A_{5k}\cos2k\theta + B_{5k}\sin2k\theta]\\ +\sin\varphi\,[C_{5k}\cos(2k-1)\theta + D_{5k}\sin(2k-1)\theta]\end{array}\right\},\qquad(15f)$$

$$\alpha_6(\theta,\varphi) = A_6 + \sum_{k=1}^{3}\{B_{6k}\cos2k\theta + C_{6k}\sin2k\theta\}.\qquad(15g)$$

Although analytical expressions for the coefficients in eqs.(15a)-(15g) have been derived in the present work, they are not provided herein due to their elaborate forms. An alternative means of evaluating these coefficients numerically was carried out instead in the implementation, as follows. Take the case of determining those coefficients of $\alpha_5(\theta,\varphi)$ as an example, where there are 12 unknowns- A_{2k}, B_{2k}, C_{2k}, , and D_{2k}, ($k = 1$, 2, or 3). One may arbitrarily prescribe 12 sample values of (θ,ϕ), followed by the numerical evaluation of the corresponding coefficients of the sextic equation. The 12 unknown coefficients may be computed by solving the 12 simultaneous equations. The same approach may be applied to determine all other coefficients of $\alpha_n(\theta,\varphi)$. Since the determination of these constants is carried out only once for a given material, the computational effort involved is relatively trivial.

It is also evident that all the partial derivatives in eqs.(11a) need also to be obtained in explicit forms for the implementation into the BEM code. Following a relatively

tedious process of algebraic manipulations, the various terms of $\hat{\Gamma}_{ij}^{(n)}$ have been derived and are shown below:

$$\hat{\Gamma}_{ij}^{(4)} = a_{ij}^{(4)} + \sum_{k=1}^{2} \left[b_{ijk}^{(4)} \cos 2k\theta + c_{ijk}^{(4)} \sin 2k\theta \right], \tag{16a}$$

$$\hat{\Gamma}_{ij}^{(3)} = a_{ij}^{(3)} \cos\varphi + \sum_{k=1}^{2} \left\{ \begin{array}{l} \cos\varphi \left[b_{ijk}^{(3)} \cos 2k\theta + c_{ijk}^{(3)} \sin 2k\theta \right] \\ + \sin\varphi \left[d_{ijk}^{(3)} \cos(2k-1)\theta + e_{ijk}^{(3)} \sin(2k-1)\theta \right] \end{array} \right\}, \tag{16b}$$

$$\begin{array}{l} \hat{\Gamma}_{ij}^{(2)} = a_{ij}^{(2)} + b_{ij}^{(2)} \cos 2\varphi + \cos^2\varphi \left[c_{ij}^{(2)} \cos 4\theta + d_{ij}^{(2)} \sin 4\varphi \right] \\ \qquad + \sin^2\varphi \left[e_{ij}^{(2)} \cos 2\theta + f_{ij}^{(2)} \sin 2\theta \right] \\ + \sum_{k=1}^{2} \left\{ \sin 2\varphi \left[g_{ijk}^{(2)} \cos(2k-1)\theta + h_{ijk}^{(2)} \sin(2k-1)\theta \right] \right\} \end{array}, \tag{16c}$$

$$\begin{array}{l} \hat{\Gamma}_{ij}^{(1)} = \cos^3\varphi \left[a_{ij}^{(1)} \cos 4\theta + b_{ij}^{(1)} \sin 4\theta \right] \\ + \cos\varphi \left[c_{ij}^{(1)} \cos 2\theta + d_{ij}^{(1)} \sin 2\theta + \cos 2\varphi \left(e_{ij}^{(1)} \cos 2\theta + f_{ij}^{(1)} \sin 2\theta \right) \right] \\ + \sin\varphi \left[\begin{array}{l} g_{ij}^{(1)} \cos\theta + h_{ij}^{(1)} \sin\theta + \cos 2\varphi \left(i_{ij}^{(1)} \cos\theta + j_{ij}^{(1)} \sin\theta \right) \\ + \cos^2\varphi \left(k_{ij}^{(1)} \cos 3\theta + l_{ij}^{(1)} \sin 3\theta \right) \end{array} \right] \end{array}, \tag{16d}$$

$$\begin{array}{l} \hat{\Gamma}_{ij}^{(0)} = a_{ij}^{(0)} + b_{ij}^{(0)} \cos 2\theta + \cos^2\varphi \sin 2\theta \left[c_{ij}^{(0)} + d_{ij}^{(0)} \cos 2\varphi \right] \\ \qquad + \cos^4\varphi \left[e_{ij}^{(0)} \cos 4\theta + f_{ij}^{(0)} \sin 4\theta \right] \\ \qquad + \cos^3\varphi \sin\varphi \left[g_{ij}^{(0)} \cos 3\theta + h_{ij}^{(0)} \sin 3\theta \right] \\ + \sum_{k=1}^{2} \left[\begin{array}{l} i_{ijk}^{(0)} \cos 2k\varphi + j_{ijk}^{(0)} \cos 2\varphi \cos 2k\theta \\ + k_{ijk}^{(0)} \cos\theta \sin 2k\theta + l_{ijk}^{(0)} \sin\theta \sin 2k\varphi \end{array} \right] \end{array} \tag{16e}$$

In eqs.(16a)-(16e), all the coefficients can be numerically computed in the same manner described above for $\alpha_n(\theta,\varphi)$. With these explicit expressions for $\hat{\Gamma}_{ij}^{(n)}$, their partial differentiations with respect to θ and ϕ may thus be obtained in a straightforward manner. For computing the 1st-order derivatives of U_{ij}, there remain the integrals in eqs.(11b) and (11c) that need to be evaluated. As derived in Lee (2009), application of Cauchy residue theorem to these integrals yields

$$\int_{-\infty}^{\infty} \frac{\hat{\Gamma}_{ij}(p) \frac{\partial f(p)}{\partial\theta}}{f^2(p)} dp = \sum_{m=0}^{5} \sum_{n=0}^{4} \hat{\Gamma}_{ij}^{(n)} \frac{\partial f_m}{\partial\theta} S_{m+n}, \tag{17a}$$

$$\int_{-\infty}^{\infty} \frac{\hat{\Gamma}_{ij}(p) \frac{\partial f(p)}{\partial\varphi}}{f^2(p)} dp = \sum_{m=0}^{5} \sum_{n=0}^{4} \hat{\Gamma}_{ij}^{(n)} \frac{\partial f_m}{\partial\varphi} S_{m+n}, \tag{17b}$$

where f_m is defined by

$$f_m = \frac{\alpha_m(\theta, \varphi)}{\alpha_6(\theta, \varphi)}, \quad (m = 0 \sim 5). \tag{18}$$

and S is given by (Lee, 2009)

$$S_n = 2\pi i \sum_{k=1}^{3} \frac{1}{(p_k - p_{k+1})^2 (p_k - p_{k+2})^2} \left[\Phi_n'(p_k) - \frac{2\Phi_n(p_k)}{(p_k - p_{k+1})} - \frac{2\Phi_n(p_k)}{(p_k - p_{k+2})} \right],$$
$$(n = 0 \sim 9), \quad (19)$$

To evaluate these integrals using eqs.(17a)-(17b), partial differentiation of f_m with respect to θ and ϕ is performed to give

$$\frac{\partial f_m}{\partial \theta} = \frac{\partial \alpha_m}{\partial \theta} \alpha_6^{-1} - \alpha_m \alpha_6^{-2} \frac{\partial \alpha_6}{\partial \theta}, \tag{20a}$$

$$\frac{\partial f_m}{\partial \varphi} = \frac{\partial \alpha_m}{\partial \varphi} \alpha_6^{-1} - \alpha_m \alpha_6^{-2} \frac{\partial \alpha_6}{\partial \varphi}. \tag{20b}$$

In eq. (20), the explicit expressions for $\partial \alpha_n / \partial \theta$ and $\partial \alpha_n / \partial \phi$ may be obtained by directly differentiating eqs. (15a)-(15g). Thus, it can be seen that all the related functions presented in the foregoing can be used to determine the 1st-order derivatives by eq. (9) without any difficulty, and no high-order tensor terms are present. The 2nd-order derivatives, required for computing stresses at internal points, will now be discussed, in the following section.

4 2nd-order derivatives of the fundamental solution for displacements

Somigliana's identity for determining the displacements at an internal point p in an elastic body may be written as

$$C_{ij} u_i(P) + \int_S u_i(Q) T_{ij}(P, Q) dS = \int_S t_i(Q) U_{ij}(P, Q) dS. \tag{21}$$

The stresses at the internal point can be found using the generalized Hooke's law

$$\sigma_{ij} = C_{ijmn} \left(u_{m,n} + u_{n,m} \right) / 2, \tag{22}$$

where the 1st-order derivatives of displacements are obtained by differentiation of eq. (21), viz,

$$C_{ij} u_i(P) + \int_S u_i(Q) T_{ij}(P, Q) dS = \int_S t_i(Q) U_{ij}(P, Q) dS. \tag{23}$$

The 1st-order derivatives of the Green's function which appear in eq. (23) have been discussed in the previous section above. From eqs.(5) and (6), it is apparent that 2nd-order derivatives of the fundamental solution will be present in $T_{ij,k}$. The expressions for the 2nd-order derivatives may be obtained using the chain rule as follows

$$\frac{\partial^2 U_{ij}}{\partial x_k \partial x_l} = \frac{\partial U_{ij,k}}{\partial r} \frac{\partial r}{\partial x_l} + \frac{\partial U_{ij,k}}{\partial \theta} \frac{\partial \theta}{\partial x_l} + \frac{\partial U_{ij,k}}{\partial \varphi} \frac{\partial \varphi}{\partial x_l} \tag{24}$$

In eq.(24), the partial differentiations of $U_{ij,k}$ with respect to the spherical coordinates are expressed as

$$\frac{\partial U_{ij,k}}{\partial r} = \frac{\partial^2 U_{ij}}{\partial r^2} \frac{\partial r}{\partial x_k} + \frac{\partial U_{ij}}{\partial r} \frac{\partial}{\partial r} \left(\frac{\partial r}{\partial x_k} \right) + \frac{\partial^2 U_{ij}}{\partial r \partial \theta} \frac{\partial \theta}{\partial x_k}$$
$$+ \frac{\partial U_{ij}}{\partial \theta} \frac{\partial}{\partial r} \left(\frac{\partial \theta}{\partial x_k} \right) + \frac{\partial^2 U_{ij}}{\partial r \partial \varphi} \frac{\partial \varphi}{\partial x_k} + \frac{\partial U_{ij}}{\partial \varphi} \frac{\partial}{\partial r} \left(\frac{\partial \varphi}{\partial x_k} \right) \tag{25a}$$

$$\frac{\partial U_{ij,k}}{\partial \theta} = \frac{\partial^2 U_{ij}}{\partial r \partial \theta} \frac{\partial r}{\partial x_k} + \frac{\partial U_{ij}}{\partial r} \frac{\partial}{\partial \theta} \left(\frac{\partial r}{\partial x_k} \right) + \frac{\partial^2 U_{ij}}{\partial \theta^2} \frac{\partial \theta}{\partial x_k}$$
$$+ \frac{\partial U_{ij}}{\partial \theta} \frac{\partial}{\partial \theta} \left(\frac{\partial \theta}{\partial x_k} \right) + \frac{\partial^2 U_{ij}}{\partial \theta \partial \varphi} \frac{\partial \varphi}{\partial x_k} + \frac{\partial U_{ij}}{\partial \varphi} \frac{\partial}{\partial \theta} \left(\frac{\partial \varphi}{\partial x_k} \right) \tag{25b}$$

$$\frac{\partial U_{ij,k}}{\partial \varphi} = \frac{\partial^2 U_{ij}}{\partial r \partial \varphi} \frac{\partial r}{\partial x_k} + \frac{\partial U_{ij}}{\partial r} \frac{\partial}{\partial \varphi} \left(\frac{\partial r}{\partial x_k} \right) + \frac{\partial^2 U_{ij}}{\partial \theta \partial \varphi} \frac{\partial \theta}{\partial x_k}$$
$$+ \frac{\partial U_{ij}}{\partial \theta} \frac{\partial}{\partial \varphi} \left(\frac{\partial \theta}{\partial x_k} \right) + \frac{\partial^2 U_{ij}}{\partial \varphi^2} \frac{\partial \varphi}{\partial x_k} + \frac{\partial U_{ij}}{\partial \varphi} \frac{\partial}{\partial \varphi} \left(\frac{\partial \varphi}{\partial x_k} \right) \tag{25c}$$

In eqs. (25a)-(25c), all 1st-order derivatives of displacements have been discussed in the previous section and $\partial \theta / \partial x_k$, $\partial \varphi / \partial x_k$ can be easily obtained (see, e.g. Lee, 2009). Differentiating U_{ij} twice with respect to the spherical coordinates r, θ, and ϕ results in the following:

$$\frac{\partial^2 U_{ij}}{\partial r^2} = \frac{U_{ij}}{r^2} - \frac{\partial U_{ij}}{\partial r}, \quad \frac{\partial^2 U_{ij}}{\partial r \partial \theta} = -\frac{1}{r^2} \frac{\partial U_{ij}}{\partial \theta}, \quad \frac{\partial^2 U_{ij}}{\partial r \partial \varphi} = -\frac{1}{r^2} \frac{\partial U_{ij}}{\partial \varphi}, \tag{26a}$$

$$\frac{\partial^2 U_{ij}}{\partial \theta^2} = \frac{1}{4\pi^2 r} \left(\frac{\partial I'_{ij}}{\partial \theta} - \frac{\partial J'_{ij}}{\partial \theta} \right),$$
$$\frac{\partial^2 U_{ij}}{\partial \varphi^2} = \frac{1}{4\pi^2 r} \left(\frac{\partial I''_{ij}}{\partial \varphi} - \frac{\partial J''_{ij}}{\partial \varphi} \right), \tag{26b}$$
$$\frac{\partial^2 U_{ij}}{\partial \theta \partial \varphi} = \frac{1}{4\pi^2 r} \left(\frac{\partial I''_{ij}}{\partial \theta} - \frac{\partial J''_{ij}}{\partial \theta} \right)$$

The task of analytically differentiating I', I'', J' and J'' with respect to θ and ϕ remains. It should be noted that eqs.(11a) and (11b) cannot be directly used to perform the partial differentiations since q_n is an implicit function of the spherical angles. The differentiations are therefore taken on their original integral forms. By differentiating the original integral form of I' with respect to θ and ϕ yields (Lee, 2009)

$$
\frac{\partial I'_{ij}}{\partial \theta} = -\frac{1}{|\boldsymbol{\kappa}|^2}\frac{\partial |\boldsymbol{\kappa}|}{\partial \theta}\int_{-\infty}^{\infty}\frac{\sum_{n=0}^{4}p^n\frac{\partial \hat{\Gamma}_{ij}^{(n)}}{\partial \theta}}{f(p)}dp + \frac{1}{|\boldsymbol{\kappa}|}\int_{-\infty}^{\infty}\left(\frac{\sum_{n=0}^{4}p^n\frac{\partial^2\hat{\Gamma}_{ij}^{(n)}}{\partial \theta^2}}{f(p)}\right)dp
$$

$$
-\frac{1}{|\boldsymbol{\kappa}|}\int_{-\infty}^{\infty}\left(\frac{\frac{\partial f(p)}{\partial \theta}\sum_{n=0}^{4}p^n\frac{\partial \hat{\Gamma}_{ij}^{(n)}}{\partial \theta}}{f^2(p)}\right)dp. \quad (27)
$$

Applying the residue theorem to the above, eq. (27) is rewritten as

$$
\frac{\partial I'_{ij}}{\partial \theta} = -\frac{1}{|\boldsymbol{\kappa}|}\left(\frac{\partial |\boldsymbol{\kappa}|}{\partial \theta}I_1 - \pi\sum_{n=0}^{4}q_n\frac{\partial^2\hat{\Gamma}_{ij}^{(n)}}{\partial \theta^2} + \sum_{m=0}^{5}\sum_{n=0}^{4}\frac{\partial \hat{\Gamma}_{ij}^{(n)}}{\partial \theta}\frac{\partial f_m}{\partial \theta}S_{m+n}\right), \quad (28)
$$

where explicit expressions for $\partial\hat{\Gamma}_{ij}^{(n)}/\partial\theta$, $\partial^2\hat{\Gamma}_{ij}^{(n)}/\partial\theta^2$ and $\partial f_m/\partial\theta$ can be analytically derived using eqs.(15a)-(15e) and eq.(20a), respectively. Similarly, partial differentiation of I'_{ij} with respect to ϕ yields

$$
\frac{\partial I'_{ij}}{\partial \phi} = -\frac{1}{|\boldsymbol{\kappa}|}\left(\frac{\partial |\boldsymbol{\kappa}|}{\partial \phi}I_1 - \pi\sum_{n=0}^{4}q_n\frac{\partial^2\hat{\Gamma}_{ij}^{(n)}}{\partial \theta \partial \phi} + \sum_{m=0}^{5}\sum_{n=0}^{4}\frac{\partial \hat{\Gamma}_{ij}^{(n)}}{\partial \theta}\frac{\partial f_m}{\partial \phi}S_{m+n}\right). \quad (29)
$$

Since $|\boldsymbol{\kappa}|$ is independent of ϕ, eq.(29) becomes

$$
\frac{\partial I'_{ij}}{\partial \phi} = \frac{1}{|\boldsymbol{\kappa}|}\left(\pi\sum_{n=0}^{4}q_n\frac{\partial^2\hat{\Gamma}_{ij}^{(n)}}{\partial \theta \partial \phi} - \sum_{m=0}^{5}\sum_{n=0}^{4}\frac{\partial \hat{\Gamma}_{ij}^{(n)}}{\partial \theta}\frac{\partial f_m}{\partial \phi}S_{m+n}\right). \quad (30)
$$

The same procedure may be applied to obtain the corresponding derivatives of I''_{ij}, the result of which are

$$
\frac{\partial I''_{ij}}{\partial \theta} = -\frac{1}{|\boldsymbol{\kappa}|}\left(\frac{\partial |\boldsymbol{\kappa}|}{\partial \theta}I''_{ij} - \pi\sum_{n=0}^{4}q_n\frac{\partial^2\hat{\Gamma}_{ij}^{(n)}}{\partial \theta \partial \phi} + \sum_{m=0}^{5}\sum_{n=0}^{4}\frac{\partial \hat{\Gamma}_{ij}^{(n)}}{\partial \phi}\frac{\partial f_m}{\partial \theta}S_{m+n}\right), \quad (31a)
$$

$$
\frac{\partial I''_{ij}}{\partial \phi} = \frac{1}{|\boldsymbol{\kappa}|}\left(\pi\sum_{n=0}^{4}q_n\frac{\partial^2\hat{\Gamma}_{ij}^{(n)}}{\partial \phi^2} - \sum_{m=0}^{5}\sum_{n=0}^{4}\frac{\partial \hat{\Gamma}_{ij}^{(n)}}{\partial \phi}\frac{\partial f_m}{\partial \phi}S_{m+n}\right). \quad (31b)
$$

Due to the presence of high-order poles, the process of differentiating J'_{ij} and J''_{ij} with respect to the two spherical angles is somewhat more involved. Using the chain rule, the partial differentiation of eq. (11b) with respect to θ gives

$$
\frac{\partial J'_{ij}}{\partial \theta} = \frac{4\pi^2 r}{|\boldsymbol{\kappa}|} \left\{ U_{ij} \left[\frac{\partial^2 |\boldsymbol{\kappa}|}{\partial \theta^2} - \frac{1}{|\boldsymbol{\kappa}|} \left(\frac{\partial |\boldsymbol{\kappa}|}{\partial \theta} \right)^2 \right] + \frac{\partial |\boldsymbol{\kappa}|}{\partial \theta} \frac{\partial U_{ij}}{\partial \theta} \right\}
$$
$$
- \frac{1}{|\boldsymbol{\kappa}|^2} \frac{\partial |\boldsymbol{\kappa}|}{\partial \theta} \int_{-\infty}^{\infty} \frac{\hat{\Gamma}_{ij}(p) \frac{\partial f(p)}{\partial \theta}}{f(p)^2} dp + \frac{1}{|\boldsymbol{\kappa}|} \int_{-\infty}^{\infty} \frac{\partial}{\partial \theta} \left[\frac{\hat{\Gamma}_{ij}(p) \frac{\partial f(p)}{\partial \theta}}{f^2(p)} \right] dp. \tag{32}
$$

In eq. (32), the first integral on the right hand side of eq.(32) has been given eq.(17a); the second one is rewritten as

$$
\int_{-\infty}^{\infty} \frac{\partial}{\partial \theta} \left(\frac{\hat{\Gamma}_{ij}(p) \frac{\partial f(p)}{\partial \theta}}{f^2(p)} \right) dp
$$
$$
= \int_{-\infty}^{\infty} \left(\frac{\frac{\partial \hat{\Gamma}_{ij}(p)}{\partial \theta} \frac{\partial f(p)}{\partial \theta} + \hat{\Gamma}_{ij}(p) \frac{\partial^2 f(p)}{\partial \theta^2}}{f^2(p)} \right) dp - 2 \int_{-\infty}^{\infty} \frac{\hat{\Gamma}_{ij}(p) \frac{\partial^2 f(p)}{\partial \theta^2}}{f^3(p)} dp. \tag{33}
$$

Applying again the residue theorem to the first integral, it becomes

$$
\int_{-\infty}^{\infty} \frac{\frac{\partial \hat{\Gamma}_{ij}(p)}{\partial \theta} \frac{\partial f(p)}{\partial \theta} + \hat{\Gamma}_{ij}(p) \frac{\partial^2 f(p)}{\partial \theta^2}}{f^2(p)} dp = \sum_{m=0}^{5} \sum_{n=0}^{4} \left[\frac{\partial \hat{\Gamma}_{ij}^{(n)}}{\partial \theta} \frac{\partial f_m}{\partial \theta} + \hat{\Gamma}_{ij}^{(n)} \frac{\partial^2 f_m}{\partial \theta^2} \right] S_{m+n}, \tag{34}
$$

where the partial derivatives of $\hat{\Gamma}_{ij}^{(n)}$ and f_m may again be readily obtained by differentiating eqs.(16a)-(16e), and eqs.(15a)-(15g) along with eq.(20a), respectively. For treating the second integral in eq.(33), consider the following integral:

$$
S'_n = \int_{-\infty}^{\infty} \frac{\Phi'_n(p)}{(p-p_1)^3 (p-p_2)^3 (p-p_3)^3} dp, \tag{35}
$$

where $\Phi'_n(p)$ is defined by

$$
\Phi'_n(p) = \frac{p^n}{(p-\bar{p}_1)^3 (p-\bar{p}_2)^3 (p-\bar{p}_3)^3}. \tag{36}
$$

Using the residue theorem for higher order poles,

$$
S'_n = 2\pi i \sum_{k=1}^{3} \frac{1}{2!} \lim_{p \to p_k} \frac{d^2}{dp^2} \left[(p-p_k)^3 \frac{\Phi'_n(p)}{(p-p_1)^3 (p-p_2)^3 (p-p_3)^3} \right]
$$
$$
= \pi i \lim_{p \to p_k} \sum_{k=1}^{3} \frac{d^2}{dp^2} \left[\sum_{j=1}^{3} \frac{\Phi'_n(p)}{(p-p_j)^3 (p-p_{j+1})^3}, \quad (p_j = p_{j-3} \text{ when } j > 3) \right],
$$

$$(37)$$

the integral of eq.(35) can then be written as

$$
S'_n = \pi i \sum_{k=1}^{3} \left\{ \frac{\frac{d^2}{dp^2}[\Phi'_n(p_k)]}{(p_k - p_{k+1})^3 (p_k - p_{k+2})^3} + \frac{6(-2p_k + p_{k+1} + p_{k+2})\frac{d}{dp}[\Phi'_n(p_k)]}{(p_k - p_{k+1})^4 (p_k - p_{k+2})^4} + \frac{6\Phi'_n(p_k)[7p_k^2 - 7p_k(p_{k+1} + p_{k+2}) + 2(p_{k+1}^2 + p_{k+2}^2)]}{(p_k - p_{k+1})^5 (p_k - p_{k+2})^5} \right\}.
$$
$$(38)$$

Further use of eq.(17a) and eqs.(32)-(34) results in

$$
\frac{\partial J'_{ij}}{\partial \theta} = \frac{4\pi^2 r}{|\boldsymbol{\kappa}|} \left\{ U_{ij} \left[\frac{\partial^2 |\boldsymbol{\kappa}|}{\partial \theta^2} - \frac{1}{|\boldsymbol{\kappa}|} \left(\frac{\partial |\boldsymbol{\kappa}|}{\partial \theta} \right)^2 \right] + \frac{\partial |\boldsymbol{\kappa}|}{\partial \theta} \frac{\partial U_{ij}}{\partial \theta} \right\}
$$
$$
- \frac{1}{|\boldsymbol{\kappa}|^2} \frac{\partial |\boldsymbol{\kappa}|}{\partial \theta} \sum_{m=0}^{5} \sum_{n=0}^{4} \hat{\Gamma}_{ij}^{(n)} \frac{\partial f_m}{\partial \theta} S_{m+n} + \frac{1}{|\boldsymbol{\kappa}|} \sum_{m=0}^{5} \sum_{n=0}^{4} \left[\frac{\partial \hat{\Gamma}_{ij}^{(n)}}{\partial \theta} \frac{\partial f_m}{\partial \theta} + \hat{\Gamma}_{ij}^{(n)} \frac{\partial^2 f_m}{\partial \theta^2} \right] S_{m+n}.
$$
$$
- \frac{2}{|\boldsymbol{\kappa}|} \sum_{m=0}^{5} \sum_{n=0}^{4} \left[\hat{\Gamma}_{ij}^{(n)} \left(\frac{\partial f_m}{\partial \theta} \right)^2 \right] S'_{m+n}
$$
$$(39)$$

In eq.(39), the term $\partial U_{ij}/\partial \theta$ has been discussed in the Section 2 for the 1st-order derivatives. Following the same procedures as described above, one may derive the expressions for $\partial J'_{ij}/\partial \varphi$, $\partial J"_{ij}/\partial \theta$, and $\partial J"_{ij}/\partial \varphi$, as

$$
\frac{\partial J'_{ij}}{\partial \varphi} = \frac{4\pi^2 r}{|\boldsymbol{\kappa}|} \frac{\partial |\boldsymbol{\kappa}|}{\partial \theta} \frac{\partial U_{ij}}{\partial \varphi} + \frac{1}{|\boldsymbol{\kappa}|} \sum_{m=0}^{5} \sum_{n=0}^{4} \left[\frac{\partial \hat{\Gamma}_{ij}^{(n)}}{\partial \varphi} \frac{\partial f_m}{\partial \theta} + \hat{\Gamma}_{ij}^{(n)} \frac{\partial^2 f_m}{\partial \theta \partial \varphi} \right] S_{m+n}
$$
$$
- \frac{2}{|\boldsymbol{\kappa}|} \sum_{m=0}^{5} \sum_{n=0}^{4} \left[\hat{\Gamma}_{ij}^{(n)} \frac{\partial f_m}{\partial \theta} \frac{\partial f_m}{\partial \varphi} \right] S'_{m+n}
$$
$$,\qquad(40a)$$

$$
\frac{\partial J"_{ij}}{\partial \theta} = -\frac{1}{|\boldsymbol{\kappa}|^2} \frac{\partial |\boldsymbol{\kappa}|}{\partial \theta} \sum_{m=0}^{5} \sum_{n=0}^{4} \hat{\Gamma}_{ij}^{(n)} \frac{\partial f_m}{\partial \phi} S_{m+n}
$$
$$
+ \frac{1}{|\boldsymbol{\kappa}|} \sum_{m=0}^{5} \sum_{n=0}^{4} \left[\frac{\partial \hat{\Gamma}_{ij}^{(n)}}{\partial \theta} \frac{\partial f_m}{\partial \phi} + \hat{\Gamma}_{ij}^{(n)} \frac{\partial^2 f_m}{\partial \phi \partial \theta} \right] S_{m+n},
$$
$$
- \frac{2}{|\boldsymbol{\kappa}|} \sum_{m=0}^{5} \sum_{n=0}^{4} \left[\hat{\Gamma}_{ij}^{(n)} \frac{\partial f_m}{\partial \phi} \frac{\partial f_m}{\partial \theta} \right] S'_{m+n}
$$
$$(40b)$$

$$\frac{\partial J''_{ij}}{\partial \varphi} = \frac{1}{|\boldsymbol{\kappa}|} \sum_{m=0}^{5} \sum_{n=0}^{4} \left[\frac{\partial \hat{\Gamma}^{(n)}_{ij}}{\partial \varphi} \frac{\partial f_m}{\partial \varphi} + \hat{\Gamma}^{(n)}_{ij} \frac{\partial^2 f_m}{\partial \varphi^2} \right] S_{m+n}$$
$$- \frac{2}{|\boldsymbol{\kappa}|} \sum_{m=0}^{5} \sum_{n=0}^{4} \left[\hat{\Gamma}^{(n)}_{ij} \left(\frac{\partial f_m}{\partial \varphi} \right)^2 \right] S'_{m+n}$$

(40c)

5   Numerical examples

Three numerical examples are presented here to demonstrate the successful implementation of the above formulations for obtaining the displacements and stresses at an interior point in a 3D anisotropic elastic body using the BEM via Somigliana's identity. In the first example, a rectangular prism of alumina crystal (Al_2O_3) is subjected to pure shear. This problem has an exact analytical solution for the displacements with which the BEM numerical solutions obtained can be verified. The second example is a niobium (*Nb*) beam subjected to a transverse distributed load. The computed displacements and stresses at its internal points are compared with a corresponding analysis using the commercial finite element method (FEM) code ANSYS. Finally, the stress concentration problem of a circular bar with a spherical cavity that was considered by the authors in Tan *et al* (2009) for the boundary solutions is re-analyzed for the displacements and stresses at points in the domain away from the cavity. The solutions are again compared with those obtained using the FEM with ANSYS.

Problem A

Figure 2(a) shows a rectangular alumina (Al_2O_3) crystal prism subjected to a uniform shear stress $\tau_{23} = \tau_o = 1$ on four of its sides. For this problem, the exact analytical solution for the displacements in the body can be found in Lekhnitskii (1963). This problem has also been treated by the present authors recently (Tan *et al*, 2009) as a test case to demonstrate the BEM implementation for its boundary solutions using the fundamental solutions of Ting and Lee (1997) and Lee (2003). In the present work, the displacements and all stress components are obtained for five arbitrarily selected points inside the prism. The elastic stiffness coefficients for the Al_2O_3 crystal are taken to be as follows (Huntington, 1958):

C_{11}= 465 GPa; C_{33}= 563 GPa; C_{44}= 233 GPa; C_{12}= 124 GPa;

C_{13}= 117 GPa; C_{14}= 101 GPa.

All the stiffness coefficients defined are arranged in accordance with the generalized stress/strain relation:

$$(\sigma_{11}\ \sigma_{22}\ \sigma_{33}\ \sigma_{23}\ \sigma_{13}\ \sigma_{12})^T = \mathbf{C}\ (\varepsilon_{11}\ \varepsilon_{22}\ \varepsilon_{33}\ \gamma_{23}\ \gamma_{13}\ \gamma_{12})^T .$$

(41)

The BEM mesh employed has 10 quadratic boundary elements with a total of 32 nodes, as shown in Fig. 2(b). Table 1 shows the comparison of all the BEM-computed displacements and stresses with analytical solutions for the sample internal points. It can be seen that the agreement of the two corresponding sets of results is excellent.
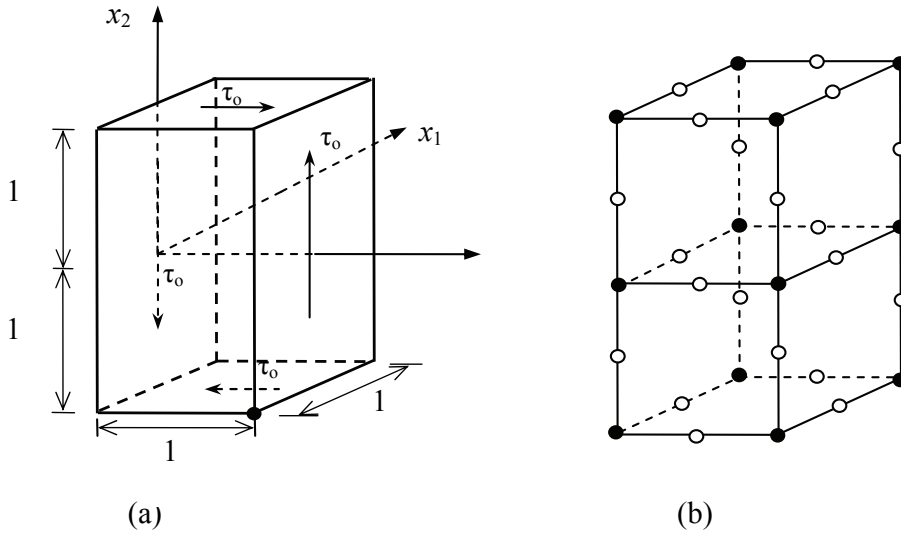
Figure 2: (a) A rectangular prism under uniform shear stress: *Problem A* (b) BEM mesh with a total of 10 elements, 32 nodes.

Problem B

In the second example, a relatively short *Nb*-crystal beam of length $12L$ with a square cross-section of side-lengths of $2L$ is subjected to a uniformly distributed pressure load, $\sigma_{22} = -P$, on its top surface. The ends of the beam are fully constrained in all the three coordinate directions. As an additional check on the implementation of the formulations, a relatively coarse BEM mesh is first used to treat an isotropic beam problem. The analysis is, however, carried out through the BEM algorithm based on the anisotropic numerical formulation, with the stiffness coefficients corresponding to an isotropic material. To allow proper comparison with the "one-dimensional" simple beam theory solution, the length of the beam should be long relative to the dimensions of the cross-section. Thus, the isotropic beam considered is one of length $24L$ instead with the same cross-section, and is subjected to the same load and end-conditions as the anisotropic

Table 1: Displacements and stresses at some internal points – *Problem A*.

	Int. point coord.	(0, 0.5, 0.5)	(0, 0.25, 0.5)	(0, 0, 0.5)	(0, -0.25, 0.5)	(0, -0.5, 0.5)
u_1	BEM	-0. 4E-09	-0. 8E-09	-0. 7E-0	-0. 1E-09	0. 8E-09
	Exact	0	0	0	0	0
u_2	BEM	0. 85522E-03	0.42762E-03	0. 19500E-07	-0. 42758E-03	-0. 85518E-03
	Exact	0.85519E-03	0. 42760E-03	0	-0. 42760E-03	-0. 85519E-03
u_3	BEM	0.28874E-02	0.14437E-02	0. 17400E-07	-0.14437E-02	-0.28874E-02
	Exact	0.28873E-02	0. 14437E-02	0	-0. 14437E-02	-0.28873E-02
σ_{11}	BEM	-0.61539E-05	-0.34317E-05	-0. 49309E-05	-0. 25667E-05	-0.47013E-05
	Exact	0	0	0	0	0
σ_{22}	BEM	0. 34529E-05	0. 38731E-05	0. 42609E-05	0. 48083E-05	0. 41356E-05
	Exact	0	0	0	0	0
σ_{33}	BEM	-0.16045E-05	-0. 8133E-06	-0. 7556E-06	-0. 23678E-05	-0. 13421E-05
	Exact	0	0	0	0	0
σ_{12}	BEM	-0. 39420E-06	0. 11470E-06	-0. 10000E-06	-0. 18560E-06	0. 27940E-06
	Exact	0	0	0	0	0
σ_{23}	BEM	1.00000	1.00000	0.999998	1.000000	1.00000
	Exact	1	1	1	1	1
σ_{13}	BEM	-0. 15336E-05	-0. 82960E-06	-0. 66590E-06	-0. 49110E-06	0. 10180E-06
	Exact	0	0	0	0	0

beam. In the numerical model, advantage is then taken about the plane of symmetry at $x_3 = 12L$ and with Poisson's ratio set to zero. The transverse displacements along the x_3-axis, at $x_3 = L, 2L,...11L$ are computed. Similarly, the longitudinal stress σ_{33} at the internal points across the sections at $x_3 = 4L$, $6L$, and $8L$, corresponding to $x_2 = \pm 0.5L, \pm 0.1L$, and $x_2 = 0$ are obtained. For comparison, the problem is also analyzed by BEM using the algorithm for 3D isotropy. Figure 3 shows the BEM mesh used for the analysis; it has 56 quadratic elements and a total of 170 boundary nodes. The computed normalized transverse x_2-displacements are shown in Figure 4(a). The longitudinal stresses, σ_{33}, across the sections at the three planes with the corresponding analytical solutions from simple beam theory can also be shown in Figure 4(b); the values at the boundary nodes in these sections are included for completeness. It can be seen that even with the relatively coarse mesh employed, very good agreement between the BEM and analytical results are obtained. The discrepancy between the results for the maximum displacement, at $x_3 = 12L$, is 4.5%, while for the maximum bending stress, at $x_3 = 0$, it is 1.7%.
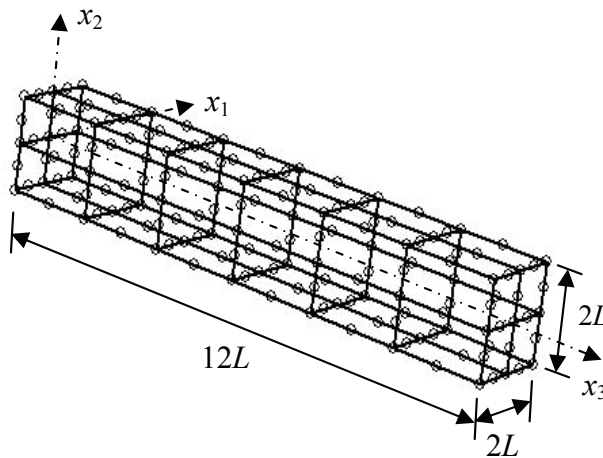
Figure 3: BEM mesh for isotropic beam analysis: *Problem B*

Next, the material for the beam is taken to be a niobium crystal which has the following elastic stiffness constants (Huntington, 1958):

$C_{11}^* = $ 246GPa; $C_{12}^* = 134$ GPa; $C_{44}^* = 28.7$ GPa,

where the asterisks denote properties defined in the directions of the principal axes of the material. For the analysis, however, these material axes are deliberately rotated successively about the global Cartesian x_1-, x_2-, and x_3-axes counterclockwise

(a)

(b)
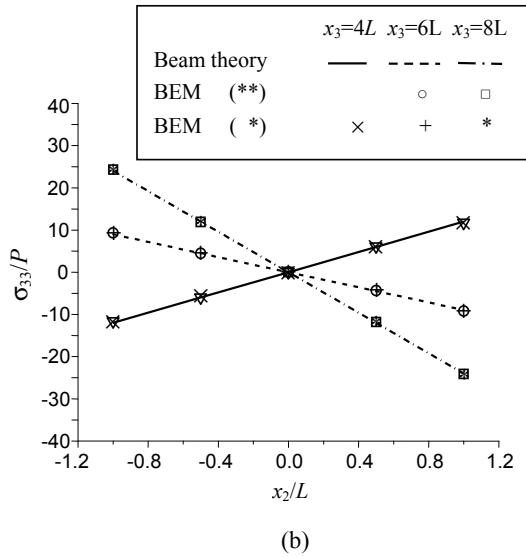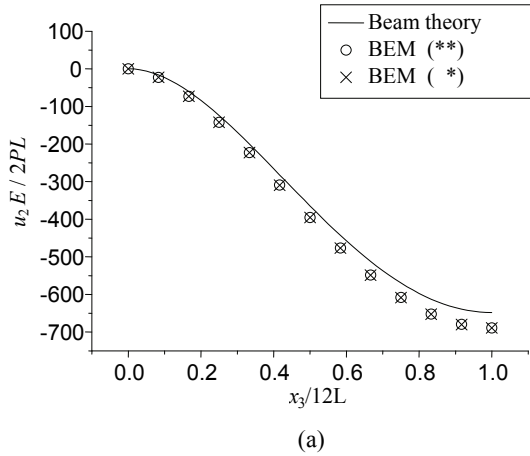
Figure 4: Isotropic beam results, *Problem B*: (a) variation of the normalized transverse (x_2-) displacements; (b) variation of the normalized normal stress. (** *anisotropic algorithm; * isotropic algorithm*)

by 15°, 30°, and 45°, respectively. This is to demonstrate the capability of the algorithm to treat general anisotropy of the material properties. The rotations of the material principal axes yield the following fully populated stiffness matrix:

$$\mathbf{C} = \begin{pmatrix} 218.7606 & 153.5152 & 141.7240 & -10.0099 & 0.4012 & 7.2133 \\ 153.5152 & 209.8947 & 150.5900 & -2.2110 & 0.9611 & -0.1750 \\ 141.7240 & 150.5900 & 221.6859 & 12.2208 & -1.3623 & -7.0383 \\ -10.0099 & -2.2110 & 12.2208 & 45.2900 & -7.0383 & 0.9611 \\ 0.4012 & 0.9611 & -1.3623 & -7.0383 & 36.4241 & -10.0099 \\ 7.2133 & -0.1750 & -7.0383 & 0.9611 & -10.0099 & 48.2152 \end{pmatrix} \text{GPa}$$

which has features of a generally anisotropic solid with respect to the global coordinate system. For verification of the BEM results, the problem was also analyzed by the FEM using the commercial code ANSYS. Of interest to note is that under this general anisotropic condition for this problem, a relatively dense mesh is found to be required for both the BEM and FEM analysis. A series of tests with increasingly refined mesh to establish convergence of the results obtained for both numerical approaches was performed. Figure 5 shows the final mesh designs used; there are 224 elements with 674 nodes for the BEM model, while for the FEM, there are 24576 SOLID186 (20-node quadratic) elements with 108545 nodes. The displacements and stresses at the same internal points as those treated in the isotropic analysis above are obtained by BEM. The computed normalized displacements along the x_3-axis of both BEM and FEM are plotted in Fig. 6 for comparison, where excellent agreement of all displacement components is observed. The results from both numerical approaches for the normalized longitudinal stresses, σ_{33}/P, and the normalized equivalent stress, σ_{eq}/P, according to von Mises criterion, across the sections at the three planes, $x_3 = 4L$, $6L$ and $8L$, are also listed in Table 2; the latter being also shown because of the presence of the other significant shear stress components due to anisotropy. The discrepancies of these results obtained from the BEM and FEM can again be seen to be very small indeed. As expected, the stresses are no longer symmetric about the x_2-axis because of the material anisotropy.

Problem C

The third problem considered is a cylindrical bar with a spherical cavity, fixed at one end and subjected to remote unit tension, $\sigma_o = 1$ at the other end, as shown in Fig. 7. With reference to this figure, two cases corresponding to $a/R = 0.4$ and 0.5, are analyzed, where a and R are the radii of the cavity and the cylindrical bar, respectively; the half-length of the bar is taken to be $H = 2R$. The material of the cylinder is taken to be the same *Nb* crystal with the material principal axes rotated by the same amounts with respect to the Cartesian axes as in *Problem B* treated above. The same fully populated elastic stiffness coefficient matrix shown earlier applies. The displacements and stresses at sample internal points around a circle of

Table 2: Variations of the normalized normal stress and von Mises equivalent stress across the sections at x_3=4L, 6L, and 8L; $x_1 = 0$.

			x_2=-L	x_2=-0.5L	x_2=0	x_2=0.5L	x_2=+L
σ_{33}/P	x_3=4L	FEM	6.5941	2.7092	-0.5490	-3.2832	-5.5895
		BEM	6.7179	2.6989	-0.5462	-3.2570	-5.7046
		|%Diff.|	1.88	0.38	0.51	0.80	2.06
	x_3=6L	FEM	8.8671	4.2660	-0.2315	-4.7287	-9.3288
		BEM	8.9934	4.2522	-0.2318	-4.7123	-9.4545
		|%Diff.|	1.42	0.32	0.13	0.35	1.35
	x_3=8L	FEM	5.1379	2.8249	0.0855	-3.1759	-7.0633
		BEM	5.2536	2.8027	0.0825	-3.1646	-7.1857
		|%Diff.|	2.25	0.79	3.51	0.36	1.73
σ_{eq}/P	x_3=4L	FEM	6.5756	3.2262	2.4541	3.4874	5.1179
		BEM	6.68	3.22	2.46	3.48	5.20
		ANSYS	8.8311	4.3283	0.4334	4.3451	8.8294
		|%Diff.|	1.57	0.13	0.09	0.17	1.68
	x_3=6L	BEM	8.9359	4.3150	0.4333	4.3323	8.9292
		|%Diff.|	1.19	0.31	0.02	0.29	1.13
	x_3=8L	FEM	5.1048	3.4532	2.4537	3.2698	6.5957
		BEM	5.1990	3.4454	2.4565	3.2654	6.6916
		|%Diff.|	1.85	0.23	0.1141	0.13	1.45

(a) (b)
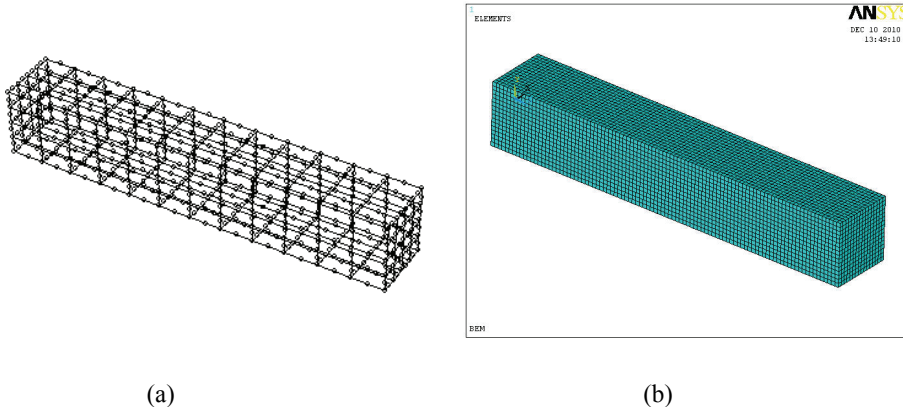
Figure 5: Numerical models for the anisotropic beam in *Problem B*: (a) BEM- 224 elements 674 nodes; (b) ANSYS- 24576 elements 108545 nodes.

relative radius $r/R = 0.75$ lying on the same plane as the equator of the cavity. Because of the presence of the various components of the displacements and stresses, the absolute resultant displacement ($\delta = \sqrt{u_1^2 + u_2^2 + u_3^2}$) and the normalized von Mises equivalent stress, σ_{eq}/σ_o, at each of these points are shown here instead. They are again compared with the corresponding values from FEM analysis using ANSYS. Figures 8(a) and 8(b) show the models employed of the both computational methods, where 88 boundary elements and 2940 SOLID186 elements are employed for the BEM and FEM analyses, respectively. These numerical results are listed in Tables 3 and 4 where, again, it can be seen that there is very good agreement indeed between the solutions obtained from both analyses.

6   Conclusions

Advances in the development of the boundary element method (BEM) for the stress analysis of three-dimensional generally anisotropic elastic solids have been relatively slow and sporadic over the past several decades. This is because of the mathematical complexity of the Green's function and its derivatives; they are required items in the BEM formulation. Based on the approach suggested by Lee (2009) very recently, an alternative, explicit algebraic form of the first and second derivatives for three-dimensional generally anisotropic elasticity have been derived and presented in this paper. They do not contain the very high order tensor terms that are present in the BEM formulation reported recently by the authors. They are also relatively simpler and computationally more efficient to evaluate in the BEM
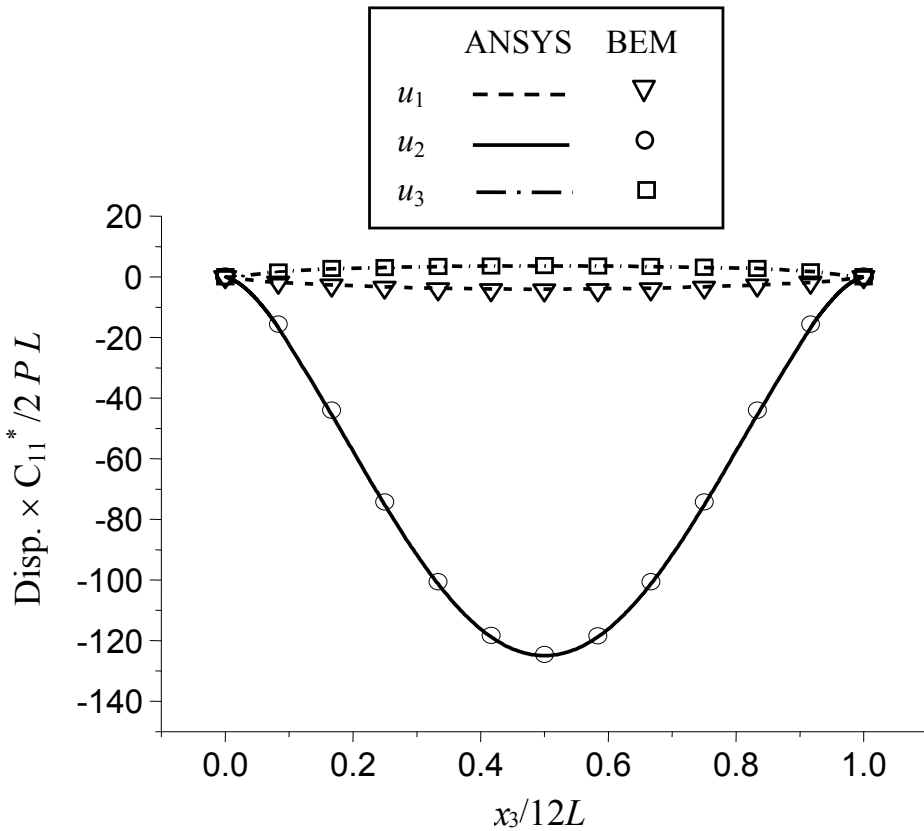
Figure 6: Variations of the normalized displacements along the x_3-axis of the anisotropic beam for *Problem B*.

implementation. Of significance is that it enables the numerical evaluation of displacements and stresses at the interior points of the three-dimensional anisotropic body using Somigliana's identity and its derivatives. These solutions are sometimes necessary at the internal points, and are carried out as a secondary procedure that is well established in BEM. The alternative formulations for the derivatives of the Green's function have been successfully implemented in the present work in BEM. Three numerical examples have been presented to demonstrate their veracity. As far as the authors are aware of, this development has never been reported previously in the literature.
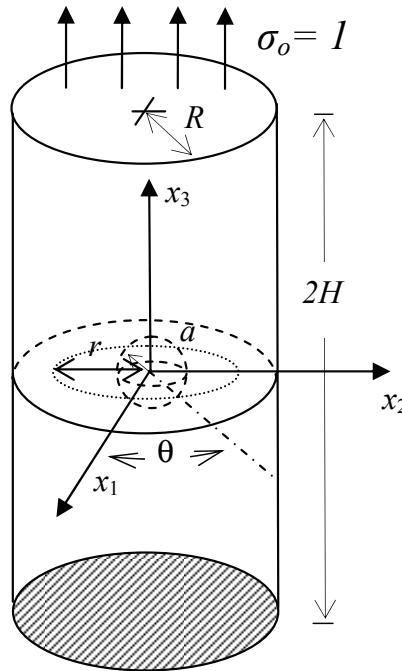
Figure 7: A cylinder with a spherical cavity under remote tension- *Problem C*.

Table 3: Resultant displacements $\delta = \sqrt{u_1^2 + u_2^2 + u_3^2}$ ($*10^{-9}$) at points on the circle at r/R =0.75 on the plane of the equator of the spherical cavity

θ	a/R=0.4			a/R=0.5		
	FEM	BEM	|%Diff.|	FEM	BEM	|%Diff.|
0^0	0.1104	0.1078	2.39	0.1240	0.1213	2.15
45^0	0.1236	0.1209	2.16	0.1390	0.1363	1.91
90^0	0.1362	0.1335	1.99	0.1529	0.1502	1.74
135^0	0.1381	0.1351	2.15	0.1562	0.1531	2.01
180^0	0.1203	0.1175	2.30	0.1349	0.1322	2.03
225^0	0.1040	0.1011	2.80	0.1161	0.1131	2.58
270^0	0.1033	0.1003	2.91	0.1167	0.1133	2.92
315^0	0.1064	0.1036	2.63	0.1200	0.1169	2.63

(a)   (b)
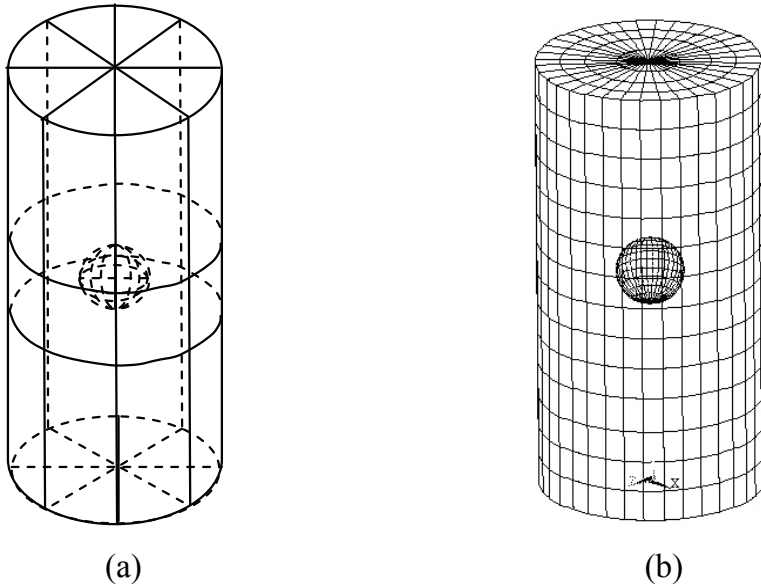
Figure 8: Mesh designs for *Problem C*: (a) 88 elements with 228 nodes for BEM; (b) 2940 SOLID186 elements with 6826 nodes for ANSYS FEM.

Table 4: Normalized von Mises equivalent stress σ_{eq}/σ_o at points on the circle at r/R =0.75 on the plane of the equator of the spherical cavity

θ	a/R=0.4			a/R=0.5		
	FEM	BEM	|%Diff.|	FEM	BEM	|%Diff.|
0^0	1.1268	1.1218	0.44	1.3093	1.3015	0.60
45^0	1.1168	1.1080	0.79	1.3036	1.2916	0.93
90^0	1.0919	1.0844	0.69	1.2722	1.2625	0.75
135^0	1.0799	1.0737	0.58	1.2881	1.2777	0.82
180^0	1.1192	1.1107	0.76	1.2989	1.2869	0.93
225^0	1.1172	1.1098	0.64	1.3063	1.2959	0.80
270^0	1.1054	1.0998	0.50	1.3022	1.2916	0.82
315^0	1.0824	1.0781	0.39	1.2899	1.2805	0.73

References

Benedetti, I.; Milazzo, A.; Aliabadi, M.H. (2009): A fast dual boundary element method for 3D anisotropic crack problems. *Int. J. Numer. Methods Engng.*, 1356-1378.

Buroni, F.C.; Saez, A. (2010): Three-dimensional Green's function and its derivative for materials with general anisotropic magneto-electro-elastic coupling. *Proc. Royal Soc. A*, 466, 515-537.

Huntington, H.B. (1958): *The Elastic Constants of Crystasl*. Academic Press, New York.

Lee,V.G. (2003): Explicit expression of derivatives of elastic Green's functions for general anisotropic materials. *Mech. Res. Comm.*, 30, 241–249.

Lee,V.G. (2009): Derivatives of the three-dimensional Green's function for anisotropic materials. *Int. J. Solids Struct., 46, 1471-1479.*

Lekhnitskii, S.G. (1963): *Theory of Elasticity of an Anisotropic Body*. Holden-Day Publishers, San Francisco.

Lifshitz, I.M.; Rosenzweig, **L.N.** (1947): Construction of the Green tensor for the fundamental equation of elasticity theory in the case of unbounded elastically anisotropic medium, *Zh. Eksp. Teor. Fiz.*, 17, 783-791.

Pan, E.; Yuan, F.G. (2000): Boundary element analysis of three dimensional cracks in anisotropic solids. *Int. J. Numer. Methods Engng.*, 48, 211-237.

Phan, P.V.; Gray, L.J.; Kaplan, T. (2004): On the residue calculus evaluation of the 3D anisotropic elastic Green's function. *Comm. Numer. Methods Engng.*, 20, 335-341.

Sales, M.A.; Gray, L.J. (1998): Evaluation of the anisotropic Green's function and its derivatives. *Comp. & Struct.*, 69, 247-254.

Schclar, N.A. (1994): *Anisotropic Analysis Using Boundary Elements*. Computational Mechanics Publications, Southampton.

Shiah, Y.C.; Tan, C.L.; Sun, W.X.; Chen, Y.H. (2010): On the displacement derivatives of the three-dimensional Green's function for generally anisotropic bodies. *Advances in Boundary Element Techniques XI*, *Proc. BeTeq 2010 Conf.*, *Berlin*, Ch. Zhang, M.H. Aliabadi & M. Schanz (eds.), E.C. Ltd. (U.K.), pp. 426-432.

Shiah, Y.C.; Tan, C.L.; Lee, V.G. (2008): Evaluation of explicit-form fundamental solutions for displacements and stresses in 3D anisotropic elastic solids. *CMES: Computer Modeling in Engineering & Sciences*, 34, 205-226.

Ting, T.C.T.; Lee,V.G. (1997):The three-dimensional elastostic Green's function for general anisotropic linear elastic solid. *Q. J. Mech. Appl. Math.*, 50, 407-426.

Tonon, F.; Pan, E.; Amadei, B. (2001): Green's functions and boundary element method formulation for 3D anisotropic media. *Comp. & Struct.*, 79, 469-482.

Wang, C.Y.; Denda, M. (2007): 3D BEM for general anisotropic elasticity. *Int. J. Solids Struct.*, 44, 7073-7091.

Wilson, R.B.; Cruse, T.A. (1978): Efficient implementation of anisotropic three dimensional boundary integral equation stress analysis. *Int. J. Numer. Methods Engng.*, 12, 1383-1397.

Appendix A Coefficients list of $|\boldsymbol{\kappa}|$

$$k_{11} = \frac{-1}{16}$$

$$\left\{
\begin{array}{l}
C_{44}\left(C_{12}^2 - C_{11}C_{22} + C_{16}^2 - 2C_{16}C_{26} + 5C_{26}^2\right) + 2C_{22}\left(C_{14}C_{56} + C_{15}C_{46}\right) \\
-4C_{45}\left[C_{16}\left(C_{22} - C_{12}\right) + C_{26}\left(C_{11} - C_{12}\right)\right] \\
+2C_{46}\left[C_{24}\left(C_{16} - 5C_{26}\right) + C_{25}\left(C_{11} - C_{12}\right)\right] \\
+C_{55}\left(C_{12}^2 - C_{11}C_{22} + 5C_{16}^2 - 2C_{16}C_{26} + C_{26}^2\right) + C_{14}^2\left(C_{22} + C_{66}\right) \\
+C_{15}^2\left(C_{22} + 5C_{66}\right) \\
+2C_{56}C_{24}\left(C_{11} - C_{12}\right) + 2C_{25}C_{56}\left(C_{16} - C_{26}\right) + C_{11}\left(C_{24}^2 + C_{25}^2\right) \\
+C_{56}^2\left(5C_{11} - 2C_{12} + C_{22}\right) + 2C_{24}\left(2C_{25}C_{16} - C_{14}C_{66}\right) \\
+C_{46}^2\left(C_{11} - 2C_{12} + 5C_{22}\right) \\
+C_{66}\left[5C_{24}^2 + C_{25}^2 + 2C_{12}(C_{44} + C_{55}) - C_{22}(5C_{44} + C_{55}) - C_{11}(C_{44} + 5C_{55})\right] \\
-2C_{14}\left[C_{26}(-2C_{15} + C_{25} - C_{46}) + C_{16}(C_{25} + C_{46}) + C_{12}(C_{24} + C_{56})\right] \\
-2C_{15}\left[C_{24}C_{26} + C_{12}(C_{25} + C_{46}) + C_{16}(C_{24} + 5C_{56}) - C_{26}C_{56} + C_{25}C_{66}\right]
\end{array}
\right\}$$

$$\text{(A.1)}$$

$$k_{21} = \frac{1}{32}$$

$$\left\{ \begin{array}{l}
C_{11}C_{25}^2 + C_{14}^2(C_{66} - C_{22}) + C_{15}^2(C_{22} + 15C_{66}) - C_{24}\left(C_{11}C_{24} + 4C_{16}C_{25}\right) \\
+ C_{44}\left(C_{16}^2 - C_{12}^2 + C_{11}C_{22} + 2C_{16}C_{26}\right) \\
+ 4C_{45}\left[C_{16}\left(C_{12} + C_{22}\right) - C_{26}\left(C_{11} + C_{12}\right)\right] \\
+ C_{55}\left(C_{12}^2 + 15C_{16}^2 - C_{11}C_{22} - 2C_{16}C_{26}\right) - C_{26}^2\left(C_{55} + 15C_{44}\right) \\
+ C_{46}\left[2C_{24}\left(15C_{26} - C_{16}\right) + 2C_{25}\left(C_{11} + C_{12}\right) + C_{46}\left(C_{11} + 2C_{12} - 15C_{22}\right)\right] \\
+ C_{56}\left[2C_{24}\left(C_{11} + C_{12}\right) + 2C_{25}\left(C_{16} + C_{26}\right) + C_{56}\left(15C_{11} - 2C_{12} - C_{22}\right)\right] \\
- C_{66}\left[15C_{24}^2 + C_{25}^2 + (C_{11} + 2C_{12} - 15C_{22})C_{44} - (-15C_{11} + 2C_{12} + C_{22})C_{55}\right] \\
+ 2C_{14}[C_{26}(2C_{15} + C_{25} - C_{46}) - C_{16}(C_{25} + C_{46}) + C_{12}(C_{24} - C_{56}) \\
- C_{22}C_{56} + C_{24}C_{66}] \\
- 2C_{15}[C_{22}C_{46} + C_{12}(C_{25} + C_{46}) - C_{26}(C_{24} + C_{56}) \\
+ C_{16}(C_{24} + 15C_{56}) + C_{25}C_{66}]
\end{array} \right\}$$

$$(A.2)$$

$$k_{22} = \frac{1}{16}$$

$$\left\{ \begin{array}{l}
C_{11}C_{24}^2 + C_{15}^2(C_{22} - 3C_{66}) + C_{14}^2(C_{22} + C_{66}) + C_{25}\left(4C_{16}C_{24} + C_{11}C_{25}\right) \\
+ C_{44}\left(C_{12}^2 + C_{16}^2 - C_{11}C_{22} - 2C_{16}C_{26} - 3C_{26}^2\right) \\
+ 4C_{45}\left[C_{16}\left(C_{12} - C_{22}\right) + C_{26}\left(C_{12} - C_{11}\right)\right] \\
+ C_{55}\left(C_{12}^2 - 3C_{16}^2 - C_{11}C_{22} - 2C_{16}C_{26} + C_{26}^2\right) \\
+ C_{46}\left[2C_{24}\left(C_{16} + 3C_{26}\right) + 2C_{25}\left(C_{11} - C_{12}\right) + C_{46}\left(C_{11} - 2C_{12} - 3C_{22}\right)\right] \\
+ C_{56}\left[2C_{24}\left(C_{11} - C_{12}\right) + 2C_{25}\left(C_{16} - C_{26}\right) - C_{56}\left(3C_{11} - 2C_{12} + C_{22}\right)\right] \\
+ C_{66}\left[-3C_{24}^2 + C_{25}^2 - C_{44}\left(C_{11} - 2C_{12} - 3C_{22}\right) + C_{55}\left(3C_{11} + 2C_{12} - C_{22}\right)\right] \\
- 2C_{14}[C_{26}(-2C_{15} + C_{25} - C_{46}) + C_{16}(C_{25} + C_{46}) - C_{22}C_{56} \\
+ C_{12}(C_{24} + C_{56}) + C_{24}C_{66}] \\
- 2C_{15}[C_{24}(C_{16} + C_{26}) - C_{22}C_{46} + C_{12}(C_{25} + C_{46}) \\
- (3C_{16} + C_{26})C_{56} + C_{25}C_{66}]
\end{array} \right\}$$

$$(A.3)$$

$$k_{23} = \frac{1}{32}$$

$$\left\{\begin{array}{l} C_{11}C_{24}^2 + C_{25}\left(4C_{16}C_{24} - C_{11}C_{25}\right) \\ + C_{44}\left(C_{12}^2 - C_{16}^2 - C_{11}C_{22} - 2C_{16}C_{26} - C_{26}^2\right) \\ + 4C_{45}\left[C_{26}\left(C_{11} + C_{12}\right) - C_{16}\left(C_{12} + C_{22}\right)\right] \\ + C_{55}\left(C_{16}^2 - C_{12}^2 + C_{11}C_{22} + 2C_{16}C_{26} + C_{26}^2\right) \\ + C_{46}\left[2C_{24}\left(C_{16} + C_{26}\right) - 2C_{25}\left(C_{11} + C_{12}\right) - C_{46}\left(C_{11} + 2C_{12} + C_{22}\right)\right] \\ - C_{56}\left[2C_{24}\left(C_{11} + C_{12}\right) + 2C_{25}\left(C_{16} + C_{26}\right) - C_{56}\left(C_{11} + 2C_{12} + C_{22}\right)\right] \\ + C_{14}^2(C_{22} - C_{66}) + C_{15}^2(-C_{22} + C_{66}) \\ + C_{66}\left[-C_{24}^2 + C_{25}^2 + (C_{11} + 2C_{12} + C_{22})(C_{44} - C_{55})\right] \\ + 2C_{14}[C_{26}(-2C_{15} - C_{25} + C_{46}) + C_{16}(C_{25} + C_{46}) + C_{22}C_{56} \\ + C_{12}(-C_{24} + C_{56}) - C_{24}\,C_{66}] \\ + 2C_{15}\left[C_{22}C_{46} + C_{12}(C_{25} + C_{46}) + C_{16}(C_{24} - C_{56}) - C_{26}(C_{24} + C_{56}) + C_{25}C_{66}\right] \end{array}\right\}$$

$$\text{(A.4)}$$

$$k_{31} = \frac{1}{16}$$

$$\left\{\begin{array}{l} C_{24}\left(5C_{16}C_{24} + 3C_{11}C_{25}\right) - C_{16}C_{25}\left(5C_{15} - 3C_{25}\right) \\ + C_{26}\left(3C_{14}^2 + 5C_{15}^2 - 3C_{15}C_{25}\right) \\ - C_{44}\left(5C_{16}C_{22} + 3C_{11}C_{26}\right) \\ + C_{45}\left(3C_{12}^2 + 5C_{16}^2 - 3C_{11}C_{22} - 6C_{16}C_{26} + 5C_{26}^2\right) \\ + C_{46}\left[3C_{11}C_{24} - C_{16}\left(5C_{15} - 3C_{25}\right) + C_{26}\left(3C_{15} - 5C_{25}\right)\right] \\ - C_{55}\left(3C_{16}C_{22} + 5C_{11}C_{26}\right) \\ + C_{56}\left[3C_{15}C_{22} + C_{24}\left(3C_{16} - 5C_{26}\right) + 5C_{11}C_{25} + 5C_{46}\left(C_{11} + C_{22}\right)\right] \\ - C_{66}\left[3C_{15}C_{24} - 5C_{24}C_{25} + 5(C_{11} + C_{22})C_{45}\right] \\ + C_{14}\left[\begin{array}{l} C_{22}\left(3C_{15} + 5C_{46}\right) - C_{24}\left(3C_{16} + 5C_{26}\right) - 3C_{12}(C_{25} + C_{46}) \\ - C_{56}\left(5C_{16} - 3C_{26}\right) + C_{66}\left(5C_{15} - 3C_{25}\right) \end{array}\right] \\ + C_{12}\left[\begin{array}{l} -C_{24}\left(3C_{15} + 5C_{46}\right) + C_{44}\left(3C_{16} + 5C_{26}\right) + C_{55}\left(5C_{16} + 3C_{26}\right) \\ - C_{56}\left(5C_{15} + 3C_{25} + 6C_{46}\right) + 6C_{45}C_{66} \end{array}\right] \end{array}\right\}$$

$$\text{(A.5)}$$

$$k_{32} = \frac{1}{4}$$

$$\left\{ \begin{array}{l} C_{26}\left(C_{12}C_{44} - C_{15}^2 - C_{14}C_{24}\right) - C_{45}\left(C_{16}^2 - C_{26}^2\right) + C_{46}\left(C_{14}C_{22} - C_{12}C_{24}\right) \\ -C_{26}\left(C_{25}C_{46} - C_{11}C_{55}\right) \\ +C_{56}\left(C_{12}C_{15} - C_{11}C_{25} - C_{24}C_{26} - C_{11}C_{46} + C_{22}C_{46}\right) \\ +C_{16}\left[C_{24}^2 - C_{22}C_{44} + C_{15}(C_{25} + C_{46}) - C_{12}C_{55} + C_{14}C_{56}\right] \\ -C_{66}\left(C_{14}C_{15} - C_{24}C_{25} - C_{11}C_{45} + C_{22}C_{45}\right) \end{array} \right\},$$

$$\text{(A.6)}$$

$$k_{33} = \frac{-1}{16}$$

$$\left\{ \begin{array}{l} C_{16}\left(C_{15}C_{25} - C_{24}^2\right) + C_{25}\left(C_{11}C_{24} + C_{16}C_{25}\right) \\ -C_{66}\left[C_{24}\left(C_{15} + C_{25}\right) - C_{45}\left(C_{11} + C_{22}\right)\right] \\ +C_{44}\left(C_{16}C_{22} - C_{11}C_{26}\right) + C_{45}\left(C_{12}^2 - C_{16}^2 - C_{11}C_{22} - 2C_{16}C_{26} - C_{26}^2\right) \\ +C_{46}\left[C_{16}\left(C_{15} + C_{25}\right) + C_{11}C_{24} + C_{26}\left(C_{15} + C_{25}\right)\right] \\ +C_{26}\left(C_{14}^2 - C_{15}^2 - C_{15}C_{25}\right) \\ -C_{55}\left(C_{16}C_{22} - C_{11}C_{26}\right) \\ +C_{56}\left[C_{15}C_{22} - C_{11}C_{25} + C_{24}\left(C_{26} + C_{16}\right) - C_{46}\left(C_{11} + C_{22}\right)\right] \\ +C_{14}[C_{22}(C_{15} - C_{46}) - C_{12}(C_{25} + C_{46}) + C_{16}(-C_{24} + C_{56}) \\ +C_{26}(C_{24} + C_{56}) - (C_{15} + C_{25})C_{66}] \\ +C_{12}[C_{24}C_{46} + (C_{16} - C_{26})(C_{44} - C_{55}) - (C_{25} + 2C_{46})C_{56} \\ +C_{15}(-C_{24} + C_{56}) + 2C_{45}C_{66}] \end{array} \right\}$$

$$\text{(A.7)}$$